How State Error Covariance Matrices Evolve in Six Dimensions

Mark A. Vincent
Raytheon

ABSTRACT

Three topics are addressed. First, the apparent paradox between Liouville's Theorem and the commonly-held concept that the state error covariance matrix is growing in time is resolved. This resolution is demonstrated for conservative systems, first for simple models and then more complex ones. Next, the non-conservative atmospheric drag force is included and the behavior over time of both the full covariance matrix and its position/velocity submatrix are examined. Finally, the implications of this behavior in calculating the Probability of Collision (Pc) of two space objects is discussed. This discussion includes why the 3-D, rather than the 2-D, method of calculating Pc is appropriate in more cases than previously thought, and why the full 7x7 covariance matrix should be used in Monte Carlo methods.

1. INTRODUCTION

The major theme of the associated paper presented at last year's AMOS conference [1] was using Keplerian or equinoctial orbital elements to calculate the Probability of Collision (Pc) between two space objects. The idea being that the Cartesian element representation did not represent the "knowledge" inherent in these alternate elements. However, after studying the literature such as Vallado's paper [2] that included the conversions for multiple representations of the covariance matrices there appeared to be a contradiction to this idea. Specifically, since the conversions could be performed in either direction at a given epoch there should not be any information "lost." This conclusion is ignoring practical issues such as machine round-off errors, singularities and the subject of one set of elements being easier to propagate accurately in time. In particular, equinoctial elements have been shown to preserve their Gaussian nature longer during the Orbit Determination (OD) itself [3, 4] and any propagations into the future. Overall, the contradiction is resolved if one considers propagating with equinoctial elements and converting to Cartesian at any chosen epoch without loss of accuracy but not *vice versa*. Also note that up to this point only 6x6 matrices have been discussed.

The importance of the off-diagonal (cross-correlation) terms was made apparent by doing a few conversions of Cartesian to Keplerian elements. A series of simple models were created to study covariance matrices under coordinate transformations and propagations in time. By first considering conservative systems, the impact of Louisville's Theorem and how it constrains the determinants of covariance and state transition matrices was examined. In particular, the apparent paradox of how covariances can "grow" but the theorem still be valid was resolved.

Within this theoretical framework, real-life data from the Orbiting Carbon Observatory-2 (OCO-2) was analyzed. The importance of the inclusion of a seventh element representing atmospheric drag was proven. From the previous analysis the appropriateness of using the determinant of the covariance, or its square root to represent a volume, was utilized. The difference in behavior of the 6x6 position/velocity submatrix and the full 7x7 including drag is significant. By using a simple rectilinear gravity model, the more important terms in the state transition matrix were determined.

In the last section the results from studying the covariance propagation behavior were applied to the calculation of the Probability of Collision (Pc). While the rigorous proof was left for future analysis, indications are that the covariance shape and size are reasons that 3-D method of calculating Pc is more appropriate than the 2-D method and why such phenomena as the peak of collision risk not occurring at the Time of Closest Approach (TCA) occur.

2. LIOUVILLE'S THEOREM

Most mechanics textbooks have a derivation and discussion of Liouville's Theorem (LT), for example pages 182-183 and 261-262 of [5]. For this initial discussion consider a conservative system with the canonical elements of Cartesian position and velocity. A finite volume bounded by the one standard deviation values of all six elements in

phase space is comprised by infinitesimal "particles." These can be considered the particles of fluid and LT states that this "phase fluid" is incompressible. Thus the volume can change in shape but its volume cannot change. As the following simple examples will illustrate, this volume can be represented by the square root of the determinant of the associated covariance matrix.

It is common knowledge and makes intuitive sense that the predicted position uncertainty for a spacecraft "grows with time" especially in the along-track component. Even with drag left out of the situation, any initial semi-major axis uncertainty translates to an along-track uncertainty at a later time, as can be derive from Kepler's 3rd law. Also, the intuitive response from most people is that there is no reason why the velocity uncertainty should be *decreasing*. Thus there appeared to be a paradox between LT and the everyday experiences that satellite operators encounter.

Perhaps the simplest model that can be used to explain away the paradox is depicted in Fig. 1 for a position X and a velocity V. The possible initial conditions at the initial time are represented by the area in the blue square Again for simplicity a constant probability distribution function (pdf) can be assumed integrating to unity over the square. It is interesting to note that Scheeres [6] introduces such a finite pdf when discussing symplectic topology and the uncertainty principle.

The extrema of the square are represented by either a positive unit value in position X^+_0 or negative unit X^-_0 with similar values for V. These extrema will be used to represent a covariance matrix in the discussion below. In this simple model there is no acceleration so the parallelogram representing the situation at time t is formed by moving all the points a distance equal to their initial velocity times t. Keeping with the unit values the figure represents movement of two time units. Elementary geometry dictates that the area of the parallelogram is equal to the area of the square.

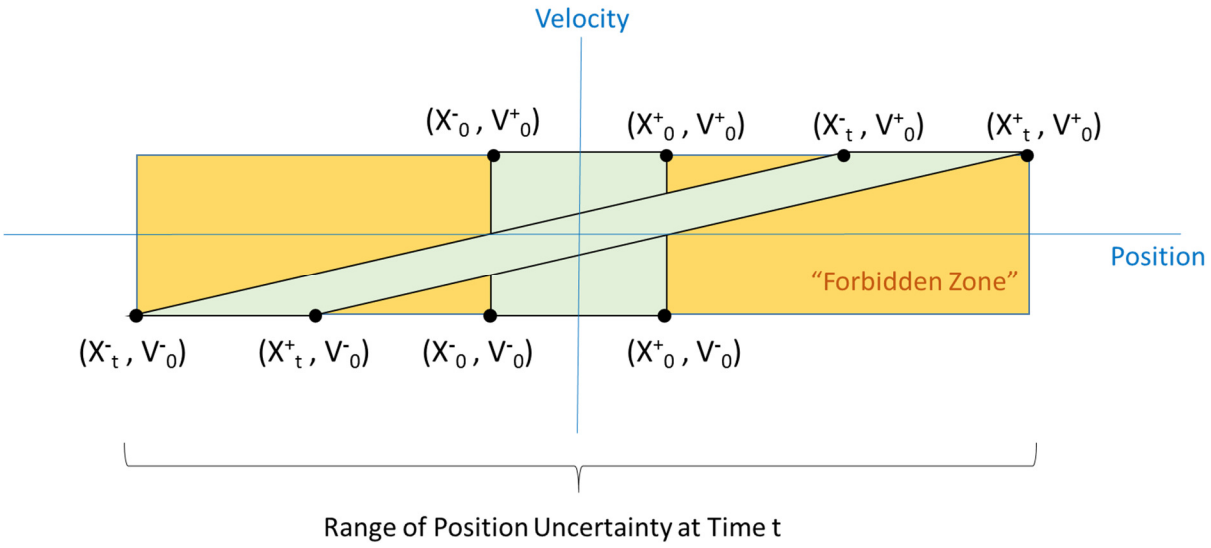

Fig. 1. Preserving Phase Space Volume in Time in the case of a Simple No-acceleration 2-D Model

As simple as the figure is, it does explain the apparent paradox. The range of possible values of position at time t certainly has grown from $X^-_0 \leftrightarrow X^+_0$ to $X^-_t \leftrightarrow X^+_t$, however the phase space area (the "volume" in 2-D) represented by either the square or parallelogram has stayed constant. The range of velocity values has remained the same. Thus, the range of position times the range of velocity (represented by the large rectangle) has grown significantly compared to the original square, however it does not represent the 'allowable" area in phase space. Conversely the area in the rectangle that is not in the square or parallelogram is not allowed in the sense the probability of being a point in that area is zero. These finite-area pdf's do not represent real-life satellite orbit uncertainties but it is a simple extension of logic to consider the allowable regions to represent higher probabilities and the forbidden areas to represent lower probabilities.

The other aspect of this simple model is that for t > 0 the position and velocity are correlated to each other. In particular, the extreme values of position had limited possible velocity values associated with them. The ramifications when calculating Pc, especially using 3-D methods is discussed later. This led to analyzing the square and parallelogram as representing covariance matrices. Although this could be considered switching from the finite pdf to an infinite one with the boundary of the two figures representing the 1-sigma standard deviations, the following analysis considers the vertices as 4 discrete points. The vertices of the square are represented by the following structure and values:

$$\begin{bmatrix} \sigma_{xo}^2 & 0 \\ 0 & \sigma_{vo}^2 \end{bmatrix} = \begin{bmatrix} 1 & 0 \\ 0 & 1 \end{bmatrix}$$

Where specifically both variances come from considering the 4 points with a mean value of $\mu = 0$ and the usual formula for the covariance:

$$1/4 \sum_{n=1}^{4} (x - \mu)^2 = (1^2 + 1^2 + 1^2 + 1^2)/4 = 1.$$

Keeping with the unit definitions for the coordinates and time, at t = 2, the vertices of the parallelogram are (1, 1), (3, 1), (-3, -1) and (-1, -1). Substituting these four points into the covariance formula give a new matrix of:

$$\begin{bmatrix} 5 & 2 \\ 2 & 1 \end{bmatrix}$$

This corresponds to the position variance growing, the velocity covariance staying the same and the introduction of the new off-diagonal covariance values. Note the determinate of the matrices remains equal to 1. Also the eigenvalues can be found to create the corresponding matrix at t= 2 of:

$$\begin{bmatrix} 3 + 2\sqrt{2} & 0 \\ 0 & 3 - 2\sqrt{2} \end{bmatrix}$$

Which of course still has a determinate equal to 1. Also note that these eigenvalues correspond to a coordinate rotation of $\pi/8 = 22.5$ degrees so the major principle axis of the parallelogram is not parallel to its long axis (which corresponds to rotation of 26.565 degrees). However, the important point is that the determinate or the square root of the determinate representing the "size of the covariance" remains constant.

Note using the square root of the determinate is consistent with the value:

$$\sqrt{(2\pi)^k \, |P|}$$

used to normalize a Gaussian pdf in k dimensions with a covariance P so the integral of all k-space give a total probability of unity.

3. LINEARIZED THEORY

As an introduction to the next section, some basic concepts of linearized theory and state transition matrices will be presented. This will also provide a basis for later discussions about the appropriateness of using linearized propagations of covariance in the calculation of Pc. Following the notation on Page 779 of Vallado's text [7], start with the non-linear relation for the time derivative of the state X:

$$\dot{\mathbf{X}} = f(\mathbf{X})$$

The linearized form of the time derivative of the state error is then:

$$\delta\dot{\mathbf{x}} = \mathbf{F}(t)\, \delta\mathbf{x} + \mathbf{u}$$

where Jacobian matrix **F**(t) is the derivative ∂f(**X**)/ ∂**X** and **u** represents the truncated higher order terms and any other unmodeled forces which are treated as process noise but will not be addressed here. The error state transition gives the relationship between the error state at time t with respect to its value at t_0 via:

$$\delta\mathbf{x} = \mathbf{\Phi}\ (t, t_0)\ \delta\mathbf{x}_0$$

and has a time derivative on Page 58 of [8]:

$$d/dt\ \mathbf{\Phi}(t, t_0) = \mathbf{F}(t)\ \mathbf{\Phi}(t, t_0)$$

If the covariance of $\delta\mathbf{x}$ at time t_k is $\mathbf{P}_k$ then the covariance at time t_{k+1} is given by:

$$\mathbf{P}_{k+1} = \mathbf{\Phi}(t_{k+1}, t_k)\ \mathbf{P}_k\ \mathbf{\Phi}(t_{k+1}, t_k)^T$$

Also, to aid in carrying on the discussion about determinants, the determinant of **Φ** is given on Page 60 of [8]:

$$|\ \mathbf{\Phi}(t, t_0)\ | = \exp\ \{\ \int_{t0}^{t} trace\ [\ \mathbf{F}(\tau)\ ]d\tau\ \}$$

known as the Jacobi-Liouville equation. Also relevant to that further discussion is the corresponding fact that if the trace of **F**(t) is zero then the determinant of **Φ** is constant.

From a different perspective, consider a generic two-variable **Φ** with elements a, b, c and d and an initial diagonal $\mathbf{P}_0$ with elements σ_1^2 and σ_2^2, then the **P** at the time represented by **Φ** is given by:

$$\mathbf{P} = \mathbf{\Phi}\ \mathbf{P}_0\ \mathbf{\Phi}^T = \begin{bmatrix} a & b \\ c & d \end{bmatrix} \begin{bmatrix} \sigma_1^2 & 0 \\ 0 & \sigma_2^2 \end{bmatrix} \begin{bmatrix} a & c \\ b & d \end{bmatrix}$$

Doing the basic matrix algebra to find **P** and its determinant gives $|\ \mathbf{P}\ | = \sigma_1^2\ \sigma_2^2\ (ad\text{-}bc)^2$. Thus the determinant of **Φ** must be +/- 1 in order for the determinant of **P** to remain constant.

4. A SIMPLE GRAVITY MODEL

A gravitational acceleration will be added to the simple model used in Section 2. It is tempting to call this "one-dimensional gravity" though a quick literature search found that that term is reserved by physicists for a one-dimensional universe. So instead think of this as the rectilinear two-body point mass problem with velocity only in the radial direction. Also, to avoid the need for absolute value signs for the position and its singularity at the origin, it will be assumed x > 0. The derivation will be similar to the 3-D case starting on Page 809 of [7] but with scalar positional and velocity terms, x and v respectively. Though note there are some discrepancies between the two derivations. The notable one is that the "jerk" term (second time derivative of the velocity) will be included here for reasons that will be apparent when discussing determinants. The second example shown here will include atmospheric drag

Simple Gravity Model without Drag

In this case the non-linear equations of motion are:

$$\dot{\mathbf{X}} = f(\mathbf{X}) = d/dt\ [x, v]^T = [\ v\ ,\ -\ \mu/x^2\ ]^T \quad \text{and} \quad \mathbf{F}(t) = \partial f(\mathbf{X})/\ \partial\mathbf{X} = \begin{bmatrix} 0 & 1 \\ 2\mu/x^3 & 0 \end{bmatrix}$$

where μ is the gravitational constant.

As explained in [7], the $\mathbf{\Phi}$ matrix is usually found by numerical integration using $\mathbf{F}$ and the identity matrix as a starting condition. Instead. here the analytical approach of using $\mathbf{\Phi} = \partial\mathbf{X}/\partial\mathbf{X}_0$ is used. In order to do this, first use a Taylor expansion in time to find the state variables to order Δt^2:

$$x = x_0 + v_0\,\Delta t - \mu/2x_0^2\,\Delta t^2$$

$$v = v_0 - \mu/x_0^2\,\Delta t + \mu v_0/x_0^3\,\Delta t^2$$

Then the terms of $\mathbf{\Phi}$ are easily derived:

$$\mathbf{\Phi} = \begin{bmatrix} 1 + \frac{\mu}{x_0^3}\Delta t^2 & \Delta t \\ \frac{2\mu}{x_0^3}\,\Delta t - \frac{3\mu}{x_0^4}\,v_0\,\Delta t^2 & 1 + \frac{\mu}{x_0^3}\,\Delta t^2 \end{bmatrix}$$

Thus to order Δt^2, the determinant of $\mathbf{\Phi} = 1$ and the covariance will remain constant as proved above (noting that this is only true because the jerk term was included). The ignored Δt^3 terms in this determinant would null this result (unless $v_0 = 0$), similarly for Δt^4, indicating all the Δt^3 and higher terms would have to be included in the Taylor expansion to keep the covariance constant to the corresponding order in Δt.

The care that must be taken in retaining like-order terms emphasizes the limited applicability of using the analytical approach for calculating $\mathbf{\Phi}$ and $\mathbf{P}$. On the other hand, if $\mathbf{\Phi}$ is integrated using $\mathbf{F}$ and a high precision integrator there is no truncation error. But to avoid confusion, note that it is the initial linearization performed in order to use $\mathbf{\Phi}$ and $\mathbf{F}$ that is challenged in the literature [3, 9], not the propagation methods of $\mathbf{\Phi}$ itself. In particular, the alternative methods either use random or carefully chosen "sigma points" about the nominal state ($\mathbf{X}$) which are then propagated using $f(\mathbf{X})$ in a non-linear manner.

The $\mathbf{F}$ matrix in this example has diagonal terms equal to zero and thus its trace is also zero which again confirms the constancy of the determinant of $\mathbf{\Phi}$. Explicitly, the time derivative of each variable does not depend on the variable itself but only on the other variable. This will not be the case when drag is introduced. The trace being zero in this no-drag conservative example also follows from Hamiltonian theory, since in that theory:

$$\dot{x} = \partial H/\partial v \;\text{ and }\; \dot{v} = -\,\partial H/\partial x$$

so the trace is:

$$\partial\dot{x}/\partial x + \partial\dot{v}/\partial v = \partial^2 H/\partial x\partial v - \partial^2 H/\partial x\partial v = 0$$

Simple Gravity Model with Drag

Using the same linear motion case but adding an atmospheric drag acceleration proportional to the velocity gives new state vector $\mathbf{X} = [\,x, v, D]$ where D is the drag factor which is assumed constant but has its own uncertainty about a nominal value (explained in detail below):

$$\dot{\mathbf{X}} = d/dt\,[x, v, D]^T = [\,v\,, -\,\mu/x^2 - D\,v|v|, 0\,]^T \quad \text{and} \quad \mathbf{F}(t) = \partial f(\mathbf{X})/\,\partial\mathbf{X} = \begin{bmatrix} 0 & 1 & 0 \\ 2\mu/x^3 & -2D|v| & -v|v| \\ 0 & 0 & 0 \end{bmatrix}$$

The term $v|v|$ is used to insure the drag acceleration is in the proper direction even if v is negative (and again $x > 0$ is assumed).

The state variables are expanded via:

$$x = x_0 + v_0\,\Delta t - \tfrac{1}{2}\,(\mu/x_0^2 + D_0\,v_0|v_0|)\,\Delta t^2$$

$$v = v_0 - (\mu/x_0^2 + D_0\, v_0|v_0|)\,\Delta t + \mu v_0/x_0^3\,\Delta t^2$$

$$D = D_0$$

Then the terms of $\mathbf{\Phi}$ are almost as easily derived:

$$\mathbf{\Phi} = \begin{bmatrix} 1 + \frac{\mu}{x_0^3}\Delta t^2 & \Delta t - 2D_0\,|v_0|\Delta t^2 & -1/2\; v_0|v_0|\;\Delta t^2 \\ \frac{2\mu}{x_0^3}\;\Delta t - \frac{3\mu}{x_0^4}\;v_0\,\Delta t^2 & 1 - 2D_0|v_0|\Delta t + \frac{\mu}{x_0^3}\;\Delta t^2 & -2v_0|v_0|\;\Delta t \\ 0 & 0 & 1 \end{bmatrix}$$

The term $-2D_0\,|v_0|\,\Delta t$ implies the determinant of $\mathbf{\Phi}$ is not constant (to order Δt). Similarly, $-2D\,|v|$ is now the trace of $\mathbf{F}$ and implies the determinant of $\mathbf{\Phi}$ is changing exponentially.

In order to examine the effect on the covariance matrix when propagating with the new $\mathbf{\Phi}$ with drag, expand the generic two-variable formulation to represent the new propagation:

$$\mathbf{P} = \mathbf{\Phi}\,\mathbf{P}_0\,\mathbf{\Phi}^{\mathbf{T}} = \begin{bmatrix} a & b & e \\ c & d & f \\ 0 & 0 & 1 \end{bmatrix} \begin{bmatrix} \sigma_x^2 & 0 & 0 \\ 0 & \sigma_v^2 & 0 \\ 0 & 0 & \sigma_D^2 \end{bmatrix} \begin{bmatrix} a & c & 0 \\ b & d & 0 \\ e & f & 1 \end{bmatrix}$$

Use the notation that $|\,\mathbf{P}_{xvD}\,|$ is the determinant of the full 3x3 covariance (analogous to a full 7x7 matrix in the non-rectilinear case), the interesting result after doing the matrix multiplications (and a lot of terms cancelling each other) is:

$$|\,\mathbf{P}_{xvD}\,| = \sigma_x^2\,\sigma_v^2\,\sigma_D^2\,(ad - bc)^2$$

That is, the "full $\mathbf{P}$ determinant" is only dependent upon the determinant of the position/velocity portion of $\mathbf{\Phi}$.

This result can also be realized using the general fact that $|\mathbf{AB}| = |\mathbf{A}|\,|\mathbf{B}|$ for arbitrary square matrices $\mathbf{A}$ and $\mathbf{B}$ [10]. This will be discussed more below after the Taylor expansion terms are substituted.

However, if $|\,\mathbf{P}_{xv}\,|$ is defined as the determinant of the position/velocity portion of $\mathbf{P}$, its value is:

$$|\,\mathbf{P}_{xv}\,| = \sigma_x^2\,\sigma_v^2\,(ad - bc)^2 + \sigma_x^2\,\sigma_D^2\,(af - ce)^2 + \sigma_v^2\,\sigma_D^2\,(bf - de)^2$$

That is, now there are three cross-terms along with their co-factor-like determinants. Note that, in general $\sigma_D^2\,|\,\mathbf{P}_{xv}\,| > |\,\mathbf{P}_{xvD}\,|$ because of all the terms are squared.

Substituting the terms from $\mathbf{\Phi}$ and retaining to order Δt^2:

$$|\,\mathbf{P}_{xvD}\,| = \sigma_x^2\,\sigma_v^2\,\sigma_D^2\,(1 - 4\,D_0\,|v_0|\,\Delta t + 4\,D_0^2\,v_0^2\,\Delta t^2)$$

$$|\,\mathbf{P}_{xv}\,| = \sigma_x^2\,\sigma_v^2\,(1 - 4\,D_0\,|v_0|\,\Delta t + 4\,D_0^2\,v_0^2\,\Delta t^2) + \sigma_x^2\,\sigma_D^2\,v_0^4\,\Delta t^2$$

At this point it is appropriate to discuss the magnitudes of the terms and the limits of the expansions. The drag factor

$$D = \tfrac{1}{2}\,\rho\,C_D\,A/M$$

where ρ is the atmospheric density, C_D is the drag coefficient, A is the effective spacecraft area and M is the spacecraft mass. The following values correspond to those of the Orbiting Carbon Observatory-2 (OCO-2) flying at 705 km whose covariance results are presented in the next section. Since the current average semi-major axis

decrease ($\dot{a}$ = 0.588 m/day = 6.81 x10^{-9} km/s) is known, it can be used to calculate the average value to use for ρ via the equation:

$$\dot{a} = - A/M\ C_D\ a^{3/2}\ \rho\ v^2 / \sqrt{\mu}$$

where μ is the gravitational constant. The value of A/M of 8.336x10^{-9} km^2/kg is used as an input to the orbit determination process. The average speed is 7.50 km/s. C_D is an estimated parameter in the OD process and a value of 1.6286 was obtained. Note, however, as is normal for OD programs, the C_D is estimated while A/M is kept fixed and the ρ comes from an independent atmospheric density model, thus any adjustment of C_D and its final uncertainty really represent adjusting the uncertainty of the product of these parameters (which will become apparent when discussing σ_D).

Substituting all the above values produces ρ = 9.46 kg/km^3. Note that this is consistent with the value from the Standard 76 atmosphere model [11] (3.0 x10^{-5} kg/km^3 at 700 km) since currently we are at a solar minimum and the standard value is averaged over the solar cycle. Using ρ produces D = 6.42 x10^{-14} /km. Note that the drag acceleration ($-Dv^2$) is -3.61x10^{-12} km/s^2. This can be compared to a gravitational acceleration of – 8.0 x10^{-3} km/s^2 at this altitude. This implies that the gravitational acceleration is over 9 orders of magnitude greater. Similarly, as discussed in the next section, σ_D is a relatively small number.

The terms containing D_0 are much smaller than the $\sigma_x^2\ \sigma_D^2\ v_0^4\ \Delta t^2$ term, especially as Δt grows. This brings up the question of how long in time this example holds. Going back to the non-drag case, Louisville's Theorem implies that $(ad - bc)^2 = 1$ independent of the Taylor expansion. So the purely gravitational terms in the drag case must also cancel each other (which follows from, for example, by considering D = 0).

The situation involving the expansion of the terms containing the drag parameter is a little more complicated. The expansion for the non-drag terms comes from the "f and g series" [12] applied to the initial conditions x_0 and v_0 (note this "f" is different than the f used in other parts of this paper). In the process of adding the drag acceleration, the fact that D is a constant (= D_0) implies that no expansion is needed for it, however the $|v|\ v$ (or in the non-rectilinear case $|\mathbf{v}|\ \mathbf{v}$) is expanded about the initial v_0 (or $\mathbf{v}_0$). In the rectilinear case, the velocity is changing relatively quickly which in turn implies the Δt must be relatively small for the expansion to be valid. However, in the non-rectilinear case if v and ρ and thus the drag acceleration magnitude is close to being constant, then the $\mathbf{\Phi}$ expansions to order Δt^2 in position and Δt is velocity can be valid for much longer periods of time. In fact, for the numerical results for a near-circular satellite shown in the next section, these expansions (which correspond to order Δt^4 in **P**) appear to be valid for at least a day in length.

5. NUMERICAL BEHAVIOR IN PHASE SPACE WITH AND WITHOUT DRAG

Before presenting numerical data from actual OCO-2 trajectories a small switch in metrics will occur. Up to this point the "size of the covariance" has been represented by the square root of the determinant of the covariance matrix. Since actual units (km^6/s^3) will be used, it seems appropriate to switch to the volume of the ellipsoid in 6 dimensions, each semi-major axis being the diagonalized standard deviation. From [13] the general volume of a n-dimensional ellipsoid is:

$$V_n = 2\pi^{n/2}\ (\sigma_1 * \sigma_2 \ldots \sigma_n)\ /\ (n\ \Gamma(n/2))$$

Substituting n = 6 and the Gamma Function value $\Gamma(3) = 2$ gives $V_6 = (\sigma_1 * \sigma_2 \ldots \sigma_6) * \pi^3/6$, thus the scale factor $\pi^3/6$ is used in all of the following 6-D results.

The following results were created by Mike Acocella using the standard process for doing the orbit determination (OD) and prediction for the OCO-2 mission. In one set of values the drag parameter was an estimated parameter (as is done for operations) and for the other it was turned off. But in both cases only the 6x6 Cartesian covariance was a standard output. The FocusLeo program was used with a 36x36 gravity field (though only a 10x10 for the "partials" presumably for both the state and covariance), luni-solar gravity and solid Earth tides. Though as discussed below, perhaps only the J_2 gravity term is important here for understanding the results.

As per the usual operational procedure, 36 hours of GPS data is used to do a batch estimation orbit determination and then state and covariance are propagated into the future as predicted values. The data supplied was for a 5.5-day prediction but the values for only a 6-hour prediction were examined and plotted. Since the estimation epoch was in the middle of 36-hour span the ends of the curves represent a 24-hour propagation from the estimation epoch (i.e. from 18 to 42 hours).

The most striking feature of Fig. 2 is that the 6x6 covariance volume (and hence the determinant) in the No Drag case remains constant, both in the OD and Prediction intervals. Thus solid proof to Louisville's Theorem. In the Drag case the volume is at a slightly higher value at the estimation epoch (18^h) than the No Drag case and then grows what appears to be quadratically in a symmetric manner backwards to 0^h and forwards to 36^h. The curve then increases in a similar manner for the 6-hour prediction period with some once per rev undulations becoming more evident.

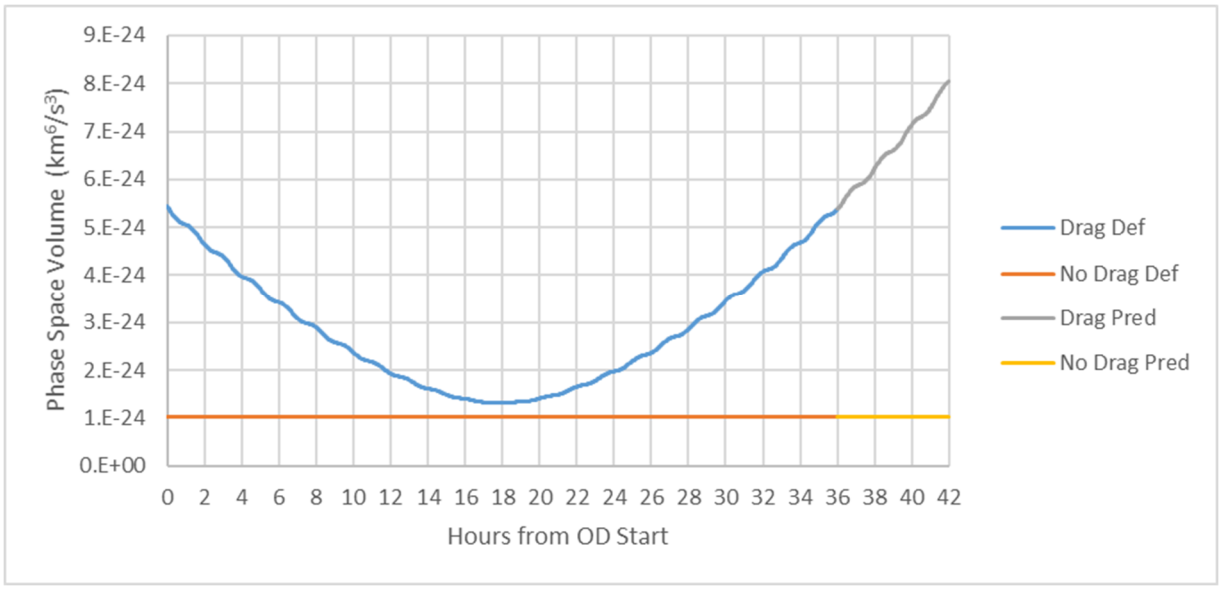

Fig. 2. Uncertainty Volume in Phase Space during (36^h) Orbit Determination and (6^h) Prediction

Below are the actual covariance matrices at the estimation epoch for the Drag and No Drag cases, that is, 18 hours after the zero epoch of 05/03 00:00:00 UTC, the symmetric matrices shown in lower triangular form:

DRAG COVARIANCE AT EPOCH = 2018-05-03T18:00:00.000
COV_REF_FRAME = EME2000
6.212253480884E-05
1.552359692477E-05 9.553580540903E-05
-1.255669530921E-05 -1.274324609494E-05 1.485175375658E-05
8.832621111077E-09 1.662915767006E-08 7.484432463627E-10 5.338143297804E-11
5.728038682283E-09 1.087137323351E-08 8.164419078869E-09 -1.576013622489E-11 2.099749856332E-11
3.187008511435E-08 7.641424360448E-08 -1.751133789422E-08 7.697469873570E-12 1.076257418097E-11 7.700244341466E-11

NO DRAG COVARIANCE AT EPOCH = 2018-05-03T18:00:00.000
COV_REF_FRAME = EME2000
5.776651546503E-05
4.357758984017E-06 6.948424094601E-05
-1.022827189167E-05 -7.249701555015E-06 1.411223497030E-05
5.551466528566E-09 1.055533477859E-08 2.347929455985E-09 5.390696774431E-11
4.612750084966E-09 7.282960443314E-09 9.236385144770E-09 -1.734213613253E-11 2.134211428608E-11
1.929120542121E-08 4.638415383901E-08 -1.131374742407E-08 8.262596231258E-14 6.888546917635E-12 4.278637275942E-11

Unfortunately, the 7x7 covariance matrix was not available at each 1-minute output step. However, the FocusLeo output summary gave the following information at the t =0, that is, the initial point in the OD are:

Estimated value of C_D = 1.6286 One-sigma Uncertainty in C_D = 1.817

Correlation Coefficients between C_D and (x, y, z, xd, yd, zd) = (0.534 0.685 0.553 -0.012 -0.596 0.735)

As discussed above, ratio of the uncertainty to the estimated value can be used with the value of D to gets its uncertainty:

$$\sigma_D = 1.817/1.6286 * 6.42 \times 10^{-14} \text{ /km} = 7.16 \times 10^{-14} \text{ /km}$$

Then the cross-correlation involving the drag can be created, for example $\sigma_{xD} = 0.534 * \sigma_x * \sigma_D$, using the correlation coefficients list above. This produces the 7x7 simulated covariance matrix:

Table 1 Simulated 7x7 Covariance Matrix

EPOCH = 2018-05-03T00:00:00.000						
1.053E-04	9.777E-05	3.119E-05	-4.838E-09	-4.291E-08	1.291E-07	3.924E-16
9.777E-05	2.369E-04	7.300E-05	-6.663E-10	-9.000E-08	2.442E-07	7.550E-16
3.119E-05	7.300E-05	3.438E-05	5.160E-09	-1.884E-08	8.205E-08	2.322E-16
-4.838E-09	-6.663E-10	5.160E-09	5.277E-11	-1.879E-11	-7.728E-12	-6.242E-21
-4.291E-08	-9.000E-08	-1.884E-08	-1.879E-11	5.363E-11	-8.984E-11	-3.125E-19
1.291E-07	2.442E-07	8.205E-08	-7.728E-12	-8.984E-11	2.785E-10	8.782E-19
3.924E-16	7.550E-16	2.322E-16	-6.242E-21	-3.125E-19	8.782E-19	5.127E-27

Note the σ_D is constant throughout both the OD and the prediction time periods, but the correlation coefficients change as the orbit evolves in Cartesian space. So having the 7x7 at one point cannot be used to verify the behavior during its propagation. Nevertheless, it (and its determinant = 2.152×10^{-76}) are useful to have in hand during the following comparison of analytical and numerical results.

The examples above for the rectilinear case assumed a diagonal initial covariance matrix. When considering a full covariance at the beginning with cross-correlation terms, the algebra becomes surprisingly cumbersome. Therefore, the gravity terms will be removed, again noting as explained above that they should disappear when taking the determinants anyway. The other small adjustment will be to substitute $1 - \Delta$ for the general variable d since as shown above it is unity plus a small number. So the new propagated covariance is:

$$\mathbf{P} = \mathbf{\Phi}\,\mathbf{P}_0\,\mathbf{\Phi}^{\mathbf{T}} = \begin{bmatrix} 1 & 0 & e \\ 0 & 1-\Delta & f \\ 0 & 0 & 1 \end{bmatrix} \begin{bmatrix} \sigma_x^2 & \sigma_{xv} & \sigma_{xD} \\ \sigma_{xv} & \sigma_v^2 & \sigma_{vD} \\ \sigma_{xD} & \sigma_{vD} & \sigma_D^2 \end{bmatrix} \begin{bmatrix} 1 & 0 & 0 \\ 0 & 1-\Delta & 0 \\ e & f & 1 \end{bmatrix}$$

Again using the fact $|\mathbf{P}| = |\mathbf{\Phi}|^2 |\mathbf{P}_0|$ it is straightforward that $|\mathbf{P}| = (1-\Delta)^2 |\mathbf{P}|$. However, the calculation of the 2x2 position/velocity determinant is more involved and after some rearrangement of terms it becomes:

$$|\mathbf{P}_{xv}| = (1-\Delta)^2 (\sigma_x^2 \sigma_v^2 - \sigma_{xv}^2) + f^2 (\sigma_x^2 \sigma_D^2 - \sigma_{xD}^2) + (1-\Delta)^2 e^2 (\sigma_v^2 \sigma_D^2 - \sigma_{vD}^2) + 2(1-\Delta) f (\sigma_x^2 \sigma_{vD} - \sigma_{xv}\sigma_{xD}) + 2(1-\Delta)^2 e (\sigma_v^2 \sigma xd - \sigma_{xv}\sigma_{vD}) + 2(1-\Delta) e*f (\sigma_{xD} \sigma_{vD} - \sigma_{xv}\sigma_D^2)$$

Which can be compared to the initial 2x2 covariance:

$$|\mathbf{P}_{xv0}| = (\sigma_x^2 \sigma_v^2 - \sigma_{xv}^2)$$

The values $e = -\frac{1}{2} v_0 |v_0| \Delta t^2$ and $f = - v_0 |v_0| \Delta t$ can be substituted into $|\mathbf{P}_{xv}|$ but it is difficult to draw any immediate conclusions about the relative size of the terms. As an empirical test, the terms were put into a spreadsheet and then a variety of correlation coefficients (and hence σ_{xv}, σ_{xD} and σ_{vD}) were used as inputs. The first observation was that both $|\mathbf{P}|$ and $|\mathbf{P}_{xv}|$ were very sensitive to these inputs. Another observation was that for $\Delta t = 86400$ seconds the e^2 term appeared to be usually the term that made $|\mathbf{P}_{xv}|$ considerably greater than $|\mathbf{P}_{xv0}|$. The square root of $|\mathbf{P}_{xv}|$ could easily be made to be an order of magnitude than the square root of $|\mathbf{P}_{xv0}|$. This increase is in line with the growth seen in Fig. 2, though, as explained earlier, drawing conclusions from the rectilinear case and applying them to the non-rectilinear case should be done with care. Nevertheless, the importance of the cross correlations has been demonstrated and should be kept in mind for such applications as Monte Carlo propagations of covariance matrices.

Another parameter to consider is the determinant (or volume) of just the position values in the real data. The volume (switching to the usual $4/3\ \pi$ as the scale factor to multiply the determinant by in 3 dimensions) for both the drag and no-drag cases are presented in Fig. 3 for the same timespan as Fig. 2.

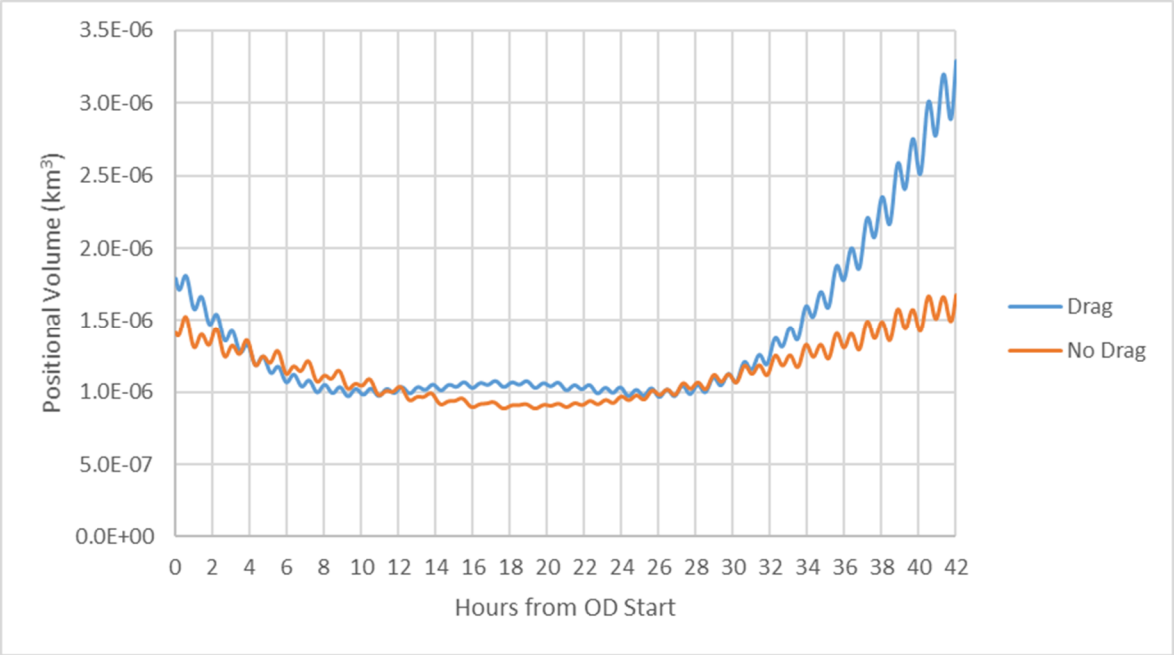

Fig. 3. Uncertainty Volume in Positional Space during Orbit Determination and Prediction

Of course, Liouville's Theorem does not apply so the curve in the no-drag case is not constant. And the growth in the prediction time span is what is usually thought of as "the uncertainty growing," especially for the drag case as a growth in along-track uncertainty. As will be discussed below, this may lead to erroneous calculations of Pc.

The non-parabolic signatures in both Figs. 2 and 3 are also of interest. In Fig. 2 the wiggles are once per rev and are likely due to the velocity-squared terms in the drag components of **F** varying as OCO-2 travels in its near-frozen (i.e. small but non-zero eccentricity) orbit. The undulations in Fig. 3 are more complicated. There is a daily period term in the drag case and both cases have twice per rev (and once per rev) wiggles. The former is probably a gravity field/drag interaction, noting that OCO-2 is in a sun-synchronous repeat orbit. The twice per day terms are likely from the J_2 gravity term. Although these terms are important (especially as the magnitude is increasing during the prediction period) for topics such as covariance scaling and any possible repercussion on Pc calculations, these topics will be addressed in future analyses.

6. RAMIFICATIONS FOR CALCULATING PROBABILITY OF COLLISION

Up to this point some interesting features of propagating 3x3, 6x6 and 7x7 covariance matrices have been demonstrated. But the implications for calculating Pc have only been hinted at. Good summaries for the 2-D methods [14] and 3-D methods [15] for calculating Pc are available in the literature. A summary of the assumptions made and how they differentiate the two methods are given below:

1. Conjunction times are short: Originally the thought was that other than the slow relative velocity cases of one satellite overtaking another or formation flying in LEO or nearby GEO orbits the 2-D assumption of a short encounter time was valid. However, that has evolved and the finite amount of time that should be considered for any conjunction has been analyzed [16].
2. Motion of the two bodies is linear during the conjunction: This assumption is a direct consequence of the short duration assumption. Hence any 3-D method that accounts for a finite conjunction period can also accommodate a curvature in the trajectories.
3. Velocity uncertainties can be ignored: In the 2-D model this assumption follows from the straight –tube implications from the other assumptions (see [14]). In the 3-D model these uncertainties can be included.
4. Covariances for the two objects are uncorrelated: Up to this point all methods make this assumption, even though the atmospheric density changes caused by solar activity is an obvious example of a correlation. Research in this area is on-going [1, 17, 18], though note the cross-correlation discussed in the latter two papers refers to that between two space objects not the cross-correlation considered here.
5. Covariances are associated with Gaussian probability distribution functions (pdf's): This topic has gathered the most attention in the past. One improvement is to have a mixture of Gaussian pdf's [19]. There is a possibility that this is tied to the time-varying covariances discussed in the next bullet. An alternative to using linearized theory and state transition matrices for propagating the error uncertainties is to use some form of sigma points integrated with the $f(t)$ matrix defined above [20]. However, the hope is that some of the analysis presented here will help clarify the distinction between the linear and non-linear techniques.
6. Covariances are fixed during the conjunction: The 3-D methods allow the covariances to change during the finite conjunction time. This allows for Pc as a function of time to be calculated and accumulated for a total Pc for the conjunction [19, 21]. However, there is little discussion of including the drag terms in the covariance matrix in these calculations. It is hoped that the following opens the door for such discussions.

Fig 4. Represents the crossing of the orbit planes of the two objects when one of the objects, call it the Primary, is at the intersection line (thus not at the nominal TCA). Consider the coupling between the (mean) semi-major axis (sma) and the along-track position (θ) of the other object, call it the Secondary. Such an isolation of these two terms has occurred in the past [9].

The same stretching of the parallelogram occurs in time for the sma and θ variables as it did in Fig. 1. Ignoring drag for the moment, being near the front of the parallelogram (velocity of course being in the same direction as θ increasing) corresponds to a lower value of sma for the Secondary at an earlier epoch, say when the propagation from an OD solution started. The two red dotes correspond to a high and low radial/sma value for the Primary. For the idealized finite "pdf inside the parallelogram" in Section2, the lower dot represents a probability of collision while the upper dot represents no possibility of collision. With real-life pdf's the lower dot represents a higher Pc and the higher dot a lower Pc. If the TCA is precisely known (or as the 2-D assumes, Pc is independent of TCA) then only probability represented by how the orbit-intersection line intersects the parallelogram is important. However, as TCA varies the orbit-intersection line crosses a different portion of the parallelogram. So even without considering drag, this simple model might explain why the 3-D differs more often than expected from the 2-D model (and why the peak Pc may occur at a time different than TCA).

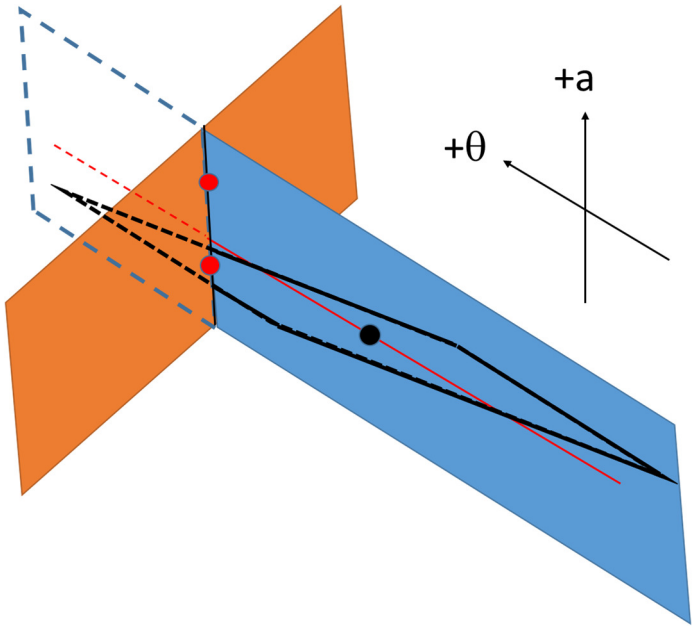

Fig. 4. How Simple Model Translates to Semi-major Axis and Along-track Components

Also analogous to this Pc dependence on geometry is the choice of direction for doing a Risk Mitigation Maneuver (RMM) as depicted in the fourth figure of [22]. That is, the coupling between sma and along-track variables imply maneuvering away from secondaries ahead and below (via an orbit raise) or behind and above (via an orbit lower) is easier than the other two quadrants. Plus, there is the operational observation that of the favorable situation of a conjunction a few days in the future where there is a medium radial separation, but small horizontal separation (i.e. the secondary is going to fly nearly directly above or below the primary). Favorable, because any reduction in the radial separation corresponding to a change in relative sma will also produce an increase in horizontal separation (analogous to the forbidden zones in Fig. 1).

It should be kept in mind that the matrix propagations in no-drag models cases above represent rotations and stretching in phase space. Thus in the 2-D model the 3x3 position covariance can be used along with the corresponding reference frame of the position and likewise for the 6x6 covariance and position and velocity for the 3-D model. What happens when drag is included is less clear. What the results above showed was that there was only a tiny decrease in the volume corresponding to a given probability in the 7x7 “extended phase space” however in the 6x6 sub-covariance for position and velocity there was a substantial increase in volume. The implications of this increase are not understood, though it does point to care when doing propagations of states using either Monte Carlo or sigma-point methods, in particular if the full 7x7 matrices need to be involved. Though as explained in [23] this may depend upon if the propagations occur from the two OD epochs or are just small (few second) variations about TCA. In particular, the “From Epoch or VCM” method of that paper corresponding to the former case do contain samples from the full covariance (also including a solar radiation parameter) in their propagations.

7. FUTURE WORK

Since all this analysis of covariance propagations, determinants and phase space volumes was somewhat of a detour from the goal of doing Pc in equinoctial elements, it is hoped to get back on track towards that goal. However, before continuing on that path, there seems to be plenty of opportunity to use the insights gained so far to study and interact with the people doing such activities as implanting the 3-D models and using Monte Carlo analysis to verify the results.

8. CONCLUSIONS

How Liouville's Theorem is valid in the conservative no-drag covariance propagation was thoroughly investigated. When drag was included, the volume in extended 7x7 phase space only decreased slightly while the volume in 6x6 position/volume phase space increased significantly in time. The ramifications of this growth in size and shape with respect to calculating the Pc of satellite conjunctions were discussed, though further examination is warranted.

9. ACKNOWLEDGEMENTS

Thank-you to Ted Sweetser for reviewing a draft of the paper and Mike Acocella for providing the OCO-2 data.

10. REFERENCES

1. Vincent, M.A., Strengthening the bridge between academia and operations for orbital debris risk mitigation, Proc. Of the Advanced Maui Optical and Space Surveillance Technologies Conference, Sept. 19-22, 2017.
2. Vallado, D.A. and Alfano, S., Updated Analytical Partials for Covariance Transformations and Optimization, 15-537, AAS/AIAA Astrodynamics Specialist Conference, Vail, CO 2015. 15-537.
3. Setty S.J., Cefola, P.J., Fielder, H., Diaz, J.F.S.J., Attributes affecting the Accuracy of a Batch Least Squares Orbit Determination using Semi-analytical Satellite Theory, Proc. of the Maui Optical and Space Surveillance Technologies Conference, Sept. 20-23, 2016.
4. Zaidi, W., Mercurio, M., Faber, W. and Schumacher, P.W., Sequential Orbit Estimation and Prediction using Modified Equinoctial Elements, AAS/ AIAA Astrodynamics Specialist Conference Paper 18-386, 19-23 Snowbird, UT, August, 2018.
5. Greenwood, D.T., *Classical Dynamics*, Prentice-Hall, 1977.
6. Scheeres, D.J., de Gosson, M.A. and Maruskin, J.M. Application of Symplectic Topology to Orbit Uncertainty and Spacecraft Navigation, J. of the Astronautical Sciences, Vol. 59, Jan-June, 2012.cheeres
7. Vallado, D.A., *Fundamentals of Astrodynamics and Applications*, 4th Edition, Microcosm Press, 2013.
8. Gelb, A., *Applied Optimal Estimation*, M.I.T. Press, 1974.
9. Alfriend, K.T. and Park. I., When does the Uncertainty become Non-Gaussian, Proc. Of the Advanced Maui Optical and Space Surveillance Technologies Conference, Sept. 20-23, 2016.
10. Noble, B., *Applied Linear Algebra*, Prentice-Hall, 1969.
11. U.S. Standard Atmosphere, 1976, NOAA, NASA, USAF, U.S. Government Printing Office, October, 1976.
12. Bate, R.B, Mueller, D.D. and White, J.E., *Fundamentals of Astrodynamics*, Dover, 1971.
13. Wilson, A.J., Volume of n-dimensional ellipsoid, Sciencia Acta Xaveriana, **1**, 2010.
14. Alfano, S., Review of Conjunction Probability Methods for Short-term Encounters, Advances in the Astronautical Sciences, **127** pp. 719-746, 2007.
15. Coppola, V.T., Including Velocity Uncertainty in the Probability of Collision between Space Objects, AAS/AIAA Space Flight Mechanics, 12-247, Charleston, South Carolina, January 29 to February 2, 2012.
16. Coppola, V.T., Evaluating the Short Encounter Assumption of the Probability of Collision Formula, AAS/AIAA Space Flight Mechanics, 12-248, Charleston, South Carolina, January 29 to February 2, 2012.
17. Coppola, V.T., Woodburn, J., and Hujsak, R., Effects of Cross Correlated Covariance on Spacecraft Collision Probability, AAS/AIAA Spaceflight Mechanics Meeting, Maui, Hawaii, Feb. 8-12, 2004.
18. Casali, S., Hall, D., Snow, D., Hejduk, M.D., Johnson, L.C., Skrehart, B.B., and Baars, L.G., Effect of Cross-Correlation of Orbital Error on Probability of Collision Determination, AAS/ AIAA Astrodynamics Specialist Conference Paper 18-272, 19-23 Snowbird, UT, August, 2018.
19. Kyle J. DeMars, Yang Cheng, and Moriba K. Jah. "Collision Probability with Gaussian Mixture Orbit Uncertainty", Journal of Guidance, Control, and Dynamics, **37**, No. 3, pp. 979-985, 2014.
20. Jones, B.A., Doostan, A., Satellite Collision Probability Estimation using Polynomial Chaos Expansion, Advances in Space Research, **52**, August, 2013.
21. Hall, D., Hejduk, M.D., Johnson, L.C., Time Dependence of Collision Probabilities during Satellite Conjunctions, AAS/AIAA Space Flight Mechanics Meeting, San Antonio, Texas, Feb. 5-9, 2017.
22. Vincent, M.A., "Bridging the Gap between Academia and Operations for Orbital Debris Risk Mitigation, Proc. of AMOS Conference," Maui, Hawaii, September 15-18, 2015.
23. Hall, D.T., Casali, S.J., Johnson, L.C., Skrehart, B.B., and Baars, L.G., High Fidelity Collision Probabilities Estimated Using Brute Force Monte Carlo Simulations, AAS/ AIAA Astrodynamics Specialist Conference Paper 18-244, 19-23 Snowbird, UT, August, 2018.